

Search for magnetic order in superconducting $\text{RuSr}_2\text{Eu}_{1.2}\text{Ce}_{0.8}\text{Cu}_2\text{O}_{10}$

J. W. Lynn,¹ Y. Chen,^{1,2} Q. Huang,¹ S. K. Goh,³ and G. V. M. Williams³

¹*NIST Center for Neutron Research, National Institute of Standards and Technology, Gaithersburg, Maryland 20899, USA*

²*Department of Materials Science and Engineering, University of Maryland, College Park, Maryland 20742, USA*

³*MacDiarmid Institute for Advanced Materials and Nanotechnology, Industrial Research, P.O. Box 31310, Lower Hutt, New Zealand*

(Received 13 December 2006; revised manuscript received 12 February 2007; published 24 July 2007)

Neutron diffraction, polarized neutron transmission, and small angle neutron scattering have been used to investigate the crystal structure and nature of the magnetic order in a polycrystalline sample of $\text{RuSr}_2\text{Eu}_{1.2}\text{Ce}_{0.8}\text{Cu}_2\text{O}_{10}$. The sample was made with the Eu-153 (98.8%) isotope to reduce the high neutron absorption for the naturally occurring element. Full refinements of the crystal structure, space group $I4/mmm$, are reported. At low temperatures only a single magnetic peak is clearly observed in a relatively wide angular range. A sharp spin reorientation transition (SRT) is observed around 35 K, close to the superconducting transition temperature ($T_c \sim 40$ K). Between the spin reorientation temperature and the Neel temperature of 59 K, additional magnetic reflections are observed. However, none of these can be simply indexed on the chemical unit cell, either as commensurate peaks or simple incommensurate magnetism, and the paucity of reflections at low T compels the conclusion that these magnetic Bragg peaks arise from an impurity phase. X-ray and neutron diffraction on the pressed pellet both show that the sample does not appear to contain substantial impurity phases, but it turns out that the magnetic impurity peaks exhibit strong preferred orientation with respect to the pellet orientation, while the primary phase does not. We have been unable to observe any magnetic order that can be identified with the ruthenate-cuprate system.

DOI: [10.1103/PhysRevB.76.014519](https://doi.org/10.1103/PhysRevB.76.014519)

PACS number(s): 74.70.Pq, 74.72.-h, 75.25.+z, 75.30.Kz

I. INTRODUCTION

The properties of the ruthenate-cuprate class of materials have been of particular interest for a decade because of the high magnetic ordering temperatures for the Ru spins, which occur well above the superconducting temperature regime.¹⁻¹⁶ The $\text{RuSr}_2\text{GdCu}_2\text{O}_8$ material (Ru1212) has been investigated in the most detail, where the Ru spins are found to order antiferromagnetically at 136 K, well above the onset of superconductivity at 40 K, while the Gd spins order antiferromagnetically at 2.5 K (Ref. 4) in a manner similar to the lanthanide magnetic order in a wide variety of cuprate superconductors.¹⁷ The properties of the $\text{RuSr}_2R_2\text{Cu}_2\text{O}_{10}$ (R = rare earth) system of direct interest here (Ru1222) have been more elusive. This system has been reported to have a larger ferromagnetic component than the Ru1212 system (which initially was also reported to be a ferromagnetic superconductor), and multiple magnetic transitions in the range from 20 K all the way up to 225 K. These various magnetic phase transitions have been difficult to interpret and understand.^{1-16,18-25}

Magnetic neutron diffraction experiments have not been reported for the Ru1222 system because of the very high neutron absorption of Eu. We therefore have undertaken neutron diffraction measurements utilizing a lower absorbing isotope of Eu, in an effort to determine the nature of the magnetic order. Initially we obtained inconsistent and confusing results, whereby we carried out a series of additional diffraction experiments as a function of temperature and magnetic field, as well as polarized neutron transmission and small angle neutron scattering measurements, in an effort to determine the origin of these problems. We discovered that the sample contained sizable single crystal impurities, that order magnetically at 59 K, and these crystals exhibit a par-

ticular orientation with respect to the axis of the cylindrical pellet. At a lower temperature of 35 K a sharp spin reorientation transition is observed, coincidentally in the vicinity of the superconducting phase transition. The majority $\text{RuSr}_2\text{Eu}_{1.2}\text{Ce}_{0.8}\text{Cu}_2\text{O}_{10}$ phase did not exhibit any preferred orientation in the powder, and that combined with the paucity of magnetic reflections at low temperature establishes that the observed magnetic ordering is not associated with this phase. Indeed we were unable to detect any magnetic ordering of the Ru moments in $\text{RuSr}_2\text{Eu}_{1.2}\text{Ce}_{0.8}\text{Cu}_2\text{O}_{10}$, which strongly suggests that many of the reports of magnetic ordering in this system actually originate from impurity phases rather than the titled compound.

II. EXPERIMENTAL DETAILS

A polycrystalline sample was prepared in the usual way⁸ in a pressed pellet form using the Eu¹⁵³ isotope to reduce the large neutron absorption from naturally occurring Eu. The pellet was approximately 1 cm in diameter and weighed ~ 1 g. The neutron absorption for Eu¹⁵³ is still quite significant, and the sample was left in pellet form for most of the measurements to reduce absorption effects as well to prevent possible rotation of the particles when a magnetic field was applied. Laboratory x-ray diffraction on the pellet indicated only small amounts of impurities.

Coarse resolution/high intensity diffraction experiments were carried out on the BT-2 and BT-7 triple axis neutron spectrometers, using pyrolytic graphite monochromator, filter, and analyzer (when employed). The neutron energy was chosen to be 14.7 meV. For the zero-field measurements the sample was sealed in helium exchange gas and placed in a closed cycle refrigerator with a low temperature capability of 4 K. Magnetic field measurements were carried out sepa-

rately in a 7 T vertical field superconducting magnet. Polarized neutron transmission measurements were carried out on BT-2 using Heusler monochromator and analyzer, again at 14.7 meV (2.359 Å). A final polarized transmission measurement on the powdered sample was carried out on the NG-1 reflectometer that employs a wavelength of 4.75 Å and supermirrors for polarizers. Small angle neutron scattering measurements were collected on the NG-1 SANS instrument using a neutron wavelength of 6 Å, collecting data over a wave vector range of 0.004 to 0.040 Å⁻¹.

High resolution powder diffraction data were collected on the BT-1 spectrometer with monochromatic neutrons of wavelength 1.5403 Å produced by a Cu(311) monochromator and 2.0775 Å with a Ge(311) monochromator. Collimators with horizontal divergences of 15', 20', and 7' arc were used before and after the monochromator, and after the sample, respectively. The intensities were measured in steps of 0.05° in the 2θ range 3°–168°. Data were collected for a variety of temperatures from 298 to 4 K to elucidate the magnetic and possible crystal structure transitions. The structural parameters were refined using the GSAS program,²⁶ using neutron scattering amplitudes of 0.822, 0.484, 0.702, 0.703, 0.772, and 0.581 (×10⁻¹² cm) for ¹⁵³Eu, Ce, Sr, Ru, Cu, and O, respectively. Initially the sample was kept in pellet form and continuously rotated to obtain the diffraction pattern, but these data were not of sufficient quality to fully refine. For the final set of diffraction measurements we crushed the pellet and enclosed the sample in a vanadium holder to obtain the data that were used in the final structural refinements.

III. RESULTS

A. Crystal structure

The structural refinements of RuSr₂Eu_{1.2}Ce_{0.8}Cu₂O_{10-δ} were carried out successfully on the powdered sample using the *I4/mmm* structural model, as shown in Fig. 1, which is isostructural with the compound RuSr₂Gd_{1.3}Ce_{0.7}Cu₂O_{10-δ}.¹⁰ Some weak impurity peaks were found and could be indexed by lattice parameters close to the SrRuO₃ and Sr₂EuRuO₆ type compounds. These phases were, therefore, taken into account in the final calculations and their inclusion significantly improved the fit. Due to the small amount of the estimated impurity phases—7.7% for the SrRuO₃-type (1:1:3) material and 5.6% for the Sr₂EuRuO₆-type double perovskite material²⁷—only lattice parameters were allowed to be refined. In particular, we do not know the specific compositions for these phases and therefore cannot relate their ordering temperatures or specific magnetic structures to our observations. We remark that it is always difficult to estimate the amount of unknown impurity phases in a sample, particularly with laboratory x-ray diffraction techniques where a detailed refinement is not carried out. This is especially true in the present case where many of the peaks of the primary and impurity phases overlap, and when investigating the pellet because of the crystalline nature of the impurities and preferred growth orientation they exhibit. These difficulties can lead to an underestimation of the actual impurity content. The structural parameters and selected interatomic distances

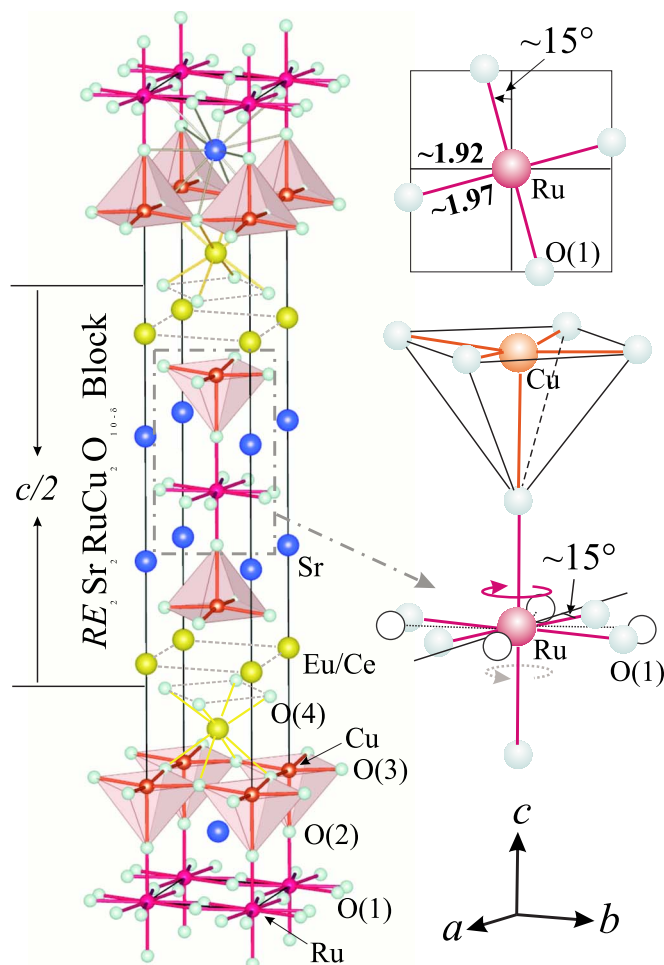


FIG. 1. (Color online) The structure for RuSr₂Eu_{1.2}Ce_{0.8}Cu₂O_{10-δ} (Ru1222). Left: structure built up by shifting the $(\frac{1}{2}, \frac{1}{2}, \frac{1}{2})$ RuSr₂Eu_{1.2}Ce_{0.8}Cu₂O_{10-δ} blocks from one another. Top-right: Rotating the RuO₆ octahedron $\sim 15^\circ$ in the *ab* plane modifies the four Ru-O in-plane distances from 1.92 to 1.97 Å to match the requirement of an average Ru-O distance ~ 1.96 Å for Ru⁴⁺-O octahedron. Bottom-right: The disordered model obtained in the refinement suggests that there is an equal number of the clockwise [darker balls of O(1)] and counterclockwise (open circles) rotations.

obtained from these neutron refinements for the primary phase are shown in Table I for two representative temperatures. Figure 2 shows a plot of the diffraction data and fit at 4 K.

No evidence of superstructures and/or orthorhombic distortions was observed. However, the large temperature factors in the *ab* plane for the in-plane oxygen atoms O(1) of the RuO₆ octahedron suggest the presence of disordered rotations. A splitting of the O(1) site from 4*c* (1/2, 0, 0) to 8*j* (1/2, *y*, 0) in the *I4/mmm* symmetry was thus modeled. We remark that the temperature factor for the apical oxygen site [O(2)] is not large, which indicates that there is no appreciable tilting, unlike that found in Ref. 10. The structure was developed, as shown in Fig. 1, by shifting the $(\frac{1}{2}, \frac{1}{2}, \frac{1}{2})$ RuSr₂Eu_{1.2}Ce_{0.8}Cu₂O_{10-δ} blocks from one another. The CuO₂ layer is then above and below the RuO₆ octahedron layer. The Cu ions are coordinated by five oxygen atoms that form

TABLE I. Structural parameters for $\text{RuEu}_{1.2}\text{Ce}_{0.8}\text{Sr}_2\text{Cu}_2\text{O}_{10-\delta}$ (in the standard crystallographic notation) at 298 and 4 K. Space group $I4/mmm$. Atomic positions are Eu/Ce $4e$ (0, 0, z), Sr $4e$ (0, 0, z), Ru $2a$ (0, 0, 0), Cu $4e$ (0, 0, z), O(1) $8j$ ($\frac{1}{2}$, y , 0), O(2) $4e$ (0, 0, z), O(3) $8g$ (0, $\frac{1}{2}$, z), and O(4) $4d$ (0, $\frac{1}{2}$, $\frac{1}{4}$).

Atom		298 K	4 K
Eu/Ce	a (Å)	3.8427(3)	3.8326(2)
	c (Å)	28.555(2)	28.485(1)
	z	0.2953(3)	0.2957(2)
	B (Å) ²	0.5(1)	0.24(7)
Sr	z	0.4227(3)	0.4219(2)
	B (Å) ²	0.98(1)	0.47(7)
Ru	B (Å) ²	0.4(2)	0.3(1)
Cu	z	0.1433(3)	0.1431(2)
	B (Å) ²	0.4(1)	0.16(6)
O(1)	y	0.117(3)	0.119(2)
	B (Å) ²	1.4(5)	1.9(3)
	Occupancy	0.45(2)	0.46(1)
O(2)	z	0.0672(3)	0.0672(2)
	B (Å) ²	0.9(2)	0.45(6)
	Occupancy	0.92(3)	0.86(1)
O(3)	z	0.1495(2)	0.1495(1)
	B (Å) ²	0.93(1)	0.80(6)
O(4)	B (Å) ²	0.8(1)	0.45(6)
	R_p (%)	4.34	4.70
	R_{wp} (%)	6.39	6.37
	χ^2	1.090	1.767

a pyramid with a longer apical Cu-O distance ~ 2.17 Å and four shorter in-plane Cu-O distances ~ 1.93 Å. The figure on the top-right in Fig. 1 shows the rotation of the RuO_6 octahedron by $\sim 15^\circ$ in the ab plane, which modifies the four

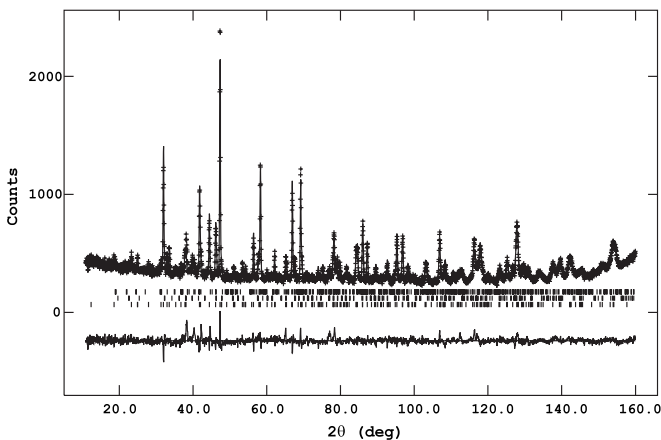


FIG. 2. Observed (crosses) and calculated (solid curve) intensity profile at 4 K. The vertical lines on the bottom indicate the angular positions for the Bragg reflections for the $\text{RuSr}_2\text{Eu}_{1.2}\text{Ce}_{0.8}\text{Cu}_2\text{O}_{10-\delta}$ system, the middle for the 1:1:3 (SrRuO_3 -like) impurity phase, and the top lines are for the $\text{Sr}_2\text{EuRuO}_6$ -like double perovskite impurity phase. The lower part of the figure shows the difference plot, $I(\text{obs})-I(\text{calc})$.

TABLE II. Calculated interatomic distances (Å) for $\text{RuEu}_{1.2}\text{Ce}_{0.8}\text{Sr}_2\text{Cu}_2\text{O}_{10-\delta}$ at 298 and 4 K. Note that the refined occupancy for O(1) and O(2) is ~ 0.9

	Number of bonds	295 K	4 K
Cu-O(2)	$\times \sim 0.9$	2.17(1)	2.162(7)
Cu-O(3)	$\times 4$	1.9294(6)	1.9237(5)
V_{Cu} (e.u.) ^a		2.27	
Ru-O(1)	$\times \sim 3.6$	1.973(3)	1.970(2)
Ru-O(2)	$\times \sim 1.8$	1.918(9)	1.915(5)
V_{Ru} (e.u.)		3.91	
Sr-O(1)	$\times \sim 3.6$	2.65(1)/3.24(1)	2.660(6)/3.253(6)
Sr-O(2)	$\times \sim 3.6$	2.733(1)	2.7876(8)
Sr-O(3)	$\times 4$	2.818(8)	2.786(4)
Eu/Ce-O(3)	$\times 4$	2.485(6)	2.479(4)
Eu/Ce-O(4)	$\times 4$	2.317(5)	2.317(5)

^aN.E. Brese and M.O'Keeffe [Acta Crystallogr., Sect. B: Struct. Sci. 47, 192 (1991)].

Ru-O in-plane distances from 1.92 to 1.97 Å to match the requirement of an average Ru-O distance ~ 1.96 Å for the Ru^{4+} -O octahedron. The figure on the lower-right shows that the disordered model obtained in the refinement, and suggests that there are an equal number of clockwise [darker balls of O(1)] and counterclockwise (open circles) rotations. The refined structural parameters reported in the Table I are rotationally averaged results.

The refined occupancies for oxygen sites [O(1) and O(2)] surrounding the Ru are $\sim 90\%$, i.e., the refined chemical formula is $\text{RuSr}_2\text{Eu}_{1.2}\text{Ce}_{0.8}\text{Cu}_2\text{O}_{9.6}$. Considering the ionic valences are 3+, 4+, 2+, and 2- for Eu, Ce, Sr, and O, respectively, the total valence for ionic Ru and 2Cu is 8.4+, in good agreement with the value of 8.45+ ($\text{Ru}^{3.91+} + 2\text{Cu}^{2.27+}$) obtained from the bond valence sum (BVS) (Ref. 28) calculations given in Table II.

In the corner-shared RuO_6 octahedra layer, the rotations of the RuO_6 octahedra are correlated, which induces superlattice parameters related to the tetragonal body-centered lattice by the transformation matrix (1, -1, 0/1, 1, 0/1, 1, 1) with $a_{\text{sup}} = \sqrt{2}a_{\text{ave}}$. The oxygen sites in the RuO_2 planes are then split into two positions with 50% occupancy for each. The presence of an oxygen vacancy can then break the correlation of the rotated RuO_6 octahedra. Figure 3 shows a proposed disordered rotational model in which the vacancies change the left-hand rotation (L) to be a right-hand rotation (R). This pattern of local displacements is similar to the pattern observed by transmission electron microscopy in the Ru1212 system, where superlattice satellites are also not observed (with x-ray diffraction).²⁹ With the present diffraction data and analysis we are not able to identify a unique rotational model.

B. Magnetic scattering

High-intensity-coarse-resolution measurements were carried out at a series of temperatures from 4 to 200 K to search

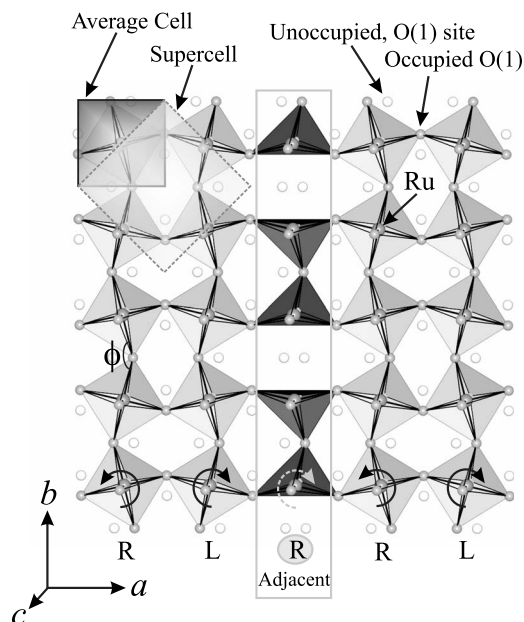


FIG. 3. A proposed local-structure model of the disordered rotation for the RuO_6 octahedral layer in $\text{RuSr}_2\text{Eu}_{1.2}\text{Ce}_{0.8}\text{Cu}_2\text{O}_{10-\delta}$ showing the relationship between the average cell and the supercell. The oxygen vacancies can change the left-hand rotation (L) into a right-hand rotation (R). The Ru-O-Ru angle ϕ is $\sim 15^\circ$.

for the development of magnetic order. The pellet was oriented to approximately bisect the incident and scattered beams, and typically the data were collected in a $\theta:2\theta$ manner. A portion of the diffraction pattern taken on BT-2 is shown in Fig. 4. The top portion of the plot shows the data obtained at 115 K, and the bottom portion of the data shows the subtraction of the 115 K data from the data collected at 5 K. In this subtraction process the paramagnetic background scattering evolves into Bragg peaks in the ordered phase, so in the subtraction there is a deficit of scattering away from the Bragg peak.³⁰ A single resolution-limited magnetic Bragg peak is observed at 42.5° indicating that long range magnetic order has developed in the sample. We remark that the scatter in the data around 50° and 60° is due to the subtraction of high intensity structural peaks which have a slight shift in their position and small change in the mean-square atomic displacements (Debye-Waller factor) with temperature, and does not originate from a magnetic order.

Figure 5 shows the magnetic scattering in detail. The low temperature magnetic peak is shown in Fig. 5(a). At the intermediate temperature of 35 K [Fig. 5(b)] we see that the peak at 42.5° has decreased dramatically in intensity, while a new peak at 39.8° and a strong peak at 45.4° have appeared, indicating an abrupt change in the magnetic structure. At 60 K [Fig. 5(c)] just a very broad distribution of magnetic scattering is observed, indicating that we are above the magnetic ordering at this temperature. No other indication of any type of magnetic order was found in the data at higher temperatures, up to 200 K.

The temperature of the magnetic transition can also be identified rather easily in the small angle neutron scattering

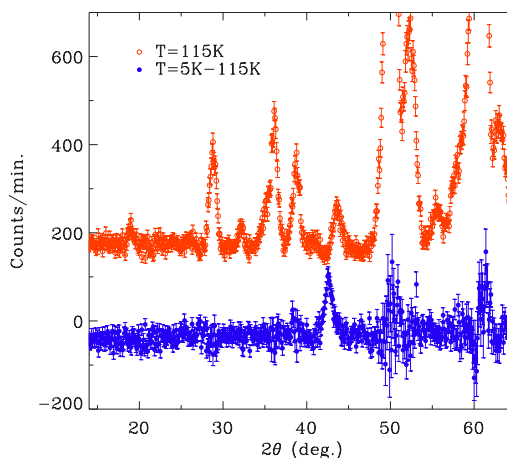


FIG. 4. (Color online) Portion of the high-intensity/coarse resolution data obtained at 115 K (top), and the magnetic diffraction pattern (bottom) obtained by subtracting these data from the data collected at 5 K. The strongest Bragg peaks are off scale so that the magnetic peak can be seen. In this subtraction process the diffuse paramagnetic scattering evolves into Bragg peaks in the ordered phase, so in the subtraction there is a deficit of scattering away from the Bragg peak.³⁰ A single resolution-limited magnetic Bragg peak is observed at 42.5° , indicating that long range magnetic order has developed in the sample. There are small changes evident in the strongest structural Bragg peaks due to the Debye-Waller factor and thermal expansion so that these intensities do not exactly subtract, but this is not evidence of any type of magnetic order (see text).

(SANS) measurements, which measure the scattering over the small wave vector part of the first Brillouin zone. Thus there is no significant variation of the atomic magnetic form factor over this wave vector range, and there is no sum rule on the overall magnetic scattering on the detector. For a ferromagnetic transition one would expect a very strong increase in the overall scattering as the transition is approached, with the increase largest in the small angle regime,³¹ and the SANS technique is in fact ideally suited for studying the scattering from ferromagnets. Figure 5(d) shows the total intensity on the SANS detector as a function of temperature, where we find a sharp decrease in scattering around 60 K, opposite to what is expected for a ferromagnet. This decrease in scattering occurs approximately uniformly over the detector, and we identify it as due to critical magnetic scattering from the antiferromagnetic ordering, which scatters neutrons at higher angles outside the range of these small wave vector measurements, and thus reduces the intensity on the SANS detector. The clear and unambiguous conclusion is that the magnetic transition is antiferromagnetic in nature, rather than ferromagnetic. No magnetic scattering other than the (weak) paramagnetic signal, and no evidence of other magnetic transitions, are observed in the SANS data over the full temperature and wave vector range explored. In particular, we did not observe any structure or additional scattering in the low q scattering below the superconducting transition temperature that would indicate the spontaneous development of vortices in the system,^{22,32} or long wavelength spin density wave states due to a competition of ferromagnetism and superconductivity.³³

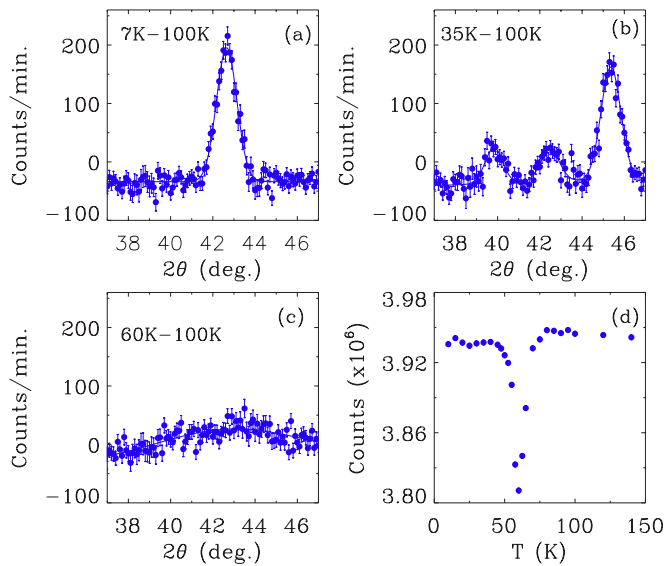


FIG. 5. (Color online) Magnetic scattering in detail. (a) Low temperature magnetic peak. (b) At 35 K the peak at 42.5° has decreased dramatically in intensity, while a new peak at 39.8° and a strong peak at 45.4° have appeared, indicating an abrupt change in the magnetic structure. (c) At 60 K only a broad distribution of magnetic scattering is observed, indicating that we are above the magnetic ordering at this temperature. (d) Total intensity observed on the small angle neutron scattering detector as a function of temperature. The sharp decrease ($\sim 3\%$) in scattering around 60 K is due to critical magnetic scattering, which depletes the incident beam and thus reduces the intensity. A ferromagnetic transition would be expected to strongly increase the scattering in the small angle regime, so we identify this transition as antiferromagnetic in nature. No other features in the SANS data are apparent over the full temperature and wave vector range explored.

The integrated intensities of the three magnetic peaks observed in Fig. 5 are shown in Fig. 6 as a function of temperature. The magnetic ordering temperature is determined to be 59 K, in excellent agreement with the SANS data. There is also a sharp (first order) spin reorientation transition around 35 K. We remark that no change in the positions of these three peaks is observed as a function of temperature.

It is instructive to compare the present results with those obtained on the related $\text{RuSr}_2\text{Gd}^{160}\text{Cu}_2\text{O}_8$ system,⁴ where there were two low angle magnetic peaks associated with the Ru magnetic order that were observed. These two peaks could be readily indexed as a simple antiferromagnetic arrangement of nearest-neighbor Ru spins, based on the chemical unit cell. This is the same magnetic structure that the Gd spins exhibit at low temperatures. The present single peak at low temperature, on the other hand, presents a problem. The observed scattering angle for this peak is much too high to correspond to any type of antiferromagnetic order of the Ru1222 material, such as with an ordering wave vector of $(1/2, 1/2, 1/2)$ as found for the Ru1212. In fact this single peak cannot be indexed in any simple way on the basis of the Ru1212 chemical unit cell. On the other hand, if the ordering were ferromagnetic, then the position of this peak would have to coincide with some structural peak, which it does not. In addition, with a ferromagnetic structure, combined

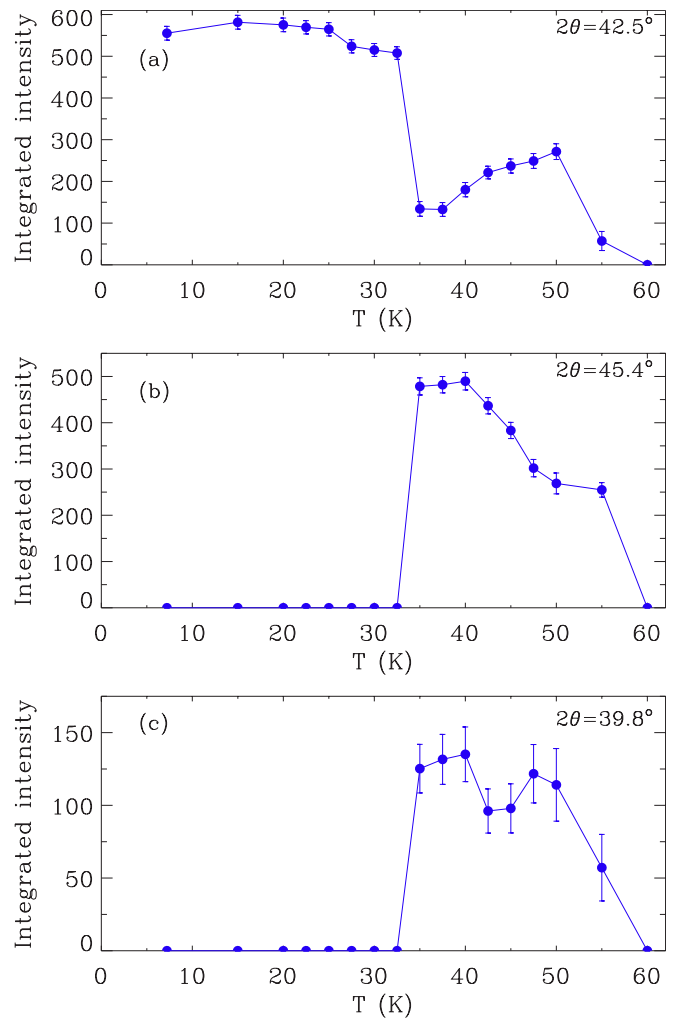


FIG. 6. (Color online) Integrated intensities of the three magnetic peaks observed in Fig. 5. The magnetic ordering temperature is determined to be 59 K. There is a sharp (first order) spin reorientation transition at 35 K. There is no change in the positions of these peaks as a function of temperature.

with the long c axis of the $\text{RuSr}_2\text{Eu}_{1.2}\text{Ce}_{0.8}\text{Cu}_2\text{O}_{10}$ structure, one would expect a series of low-angle magnetic peaks indexed as $q=(0,0,2l)$, starting at an angle of $\sim 9.5^\circ$ and (approximate) multiples. Since none of these low-angle peaks is observed, the only way to explain their absence based on the $\text{RuSr}_2\text{Eu}_{1.2}\text{Ce}_{0.8}\text{Cu}_2\text{O}_{10}$ crystal structure is to assume that the magnetic moments point along the c axis; the magnetic intensities are proportional to

$$I \propto 1 - (\hat{q} \cdot \hat{M})^2,$$

where \hat{q} and \hat{M} are unit vectors in the direction of the reciprocal lattice vector and spin direction, respectively, and with the moments parallel to the c axis the intensities would be extinguished for these reflections. However, there would still be additional (h,k,l) reflections with nonzero h, k that must be present but are not observed. Thus a ferromagnetic structure or any type of commensurate antiferromagnetic structure for $\text{RuSr}_2\text{Eu}_{1.2}\text{Ce}_{0.8}\text{Cu}_2\text{O}_{10}$ can be unambiguously ruled out

as giving rise to the observed magnetic peak. For an incommensurate magnetic structure, on the other hand, equally spaced satellite peaks about the structural peaks should be observed, so that we should see even more magnetic peaks than in the case of a commensurate magnetic structure.³⁴ We can therefore also rule out an incommensurate magnetic structure as the origin of this lone magnetic Bragg reflection, and are irrevocably led to the conclusion that this peak must originate from an impurity phase.

An additional difficulty that occurred in the diffraction measurements is that the intensity of the magnetic peak at low temperatures could be quite different from one thermal cycling to the next, or from one experiment to the next. Initially it was thought that the thermal path taken to low temperature was indeed an important factor, but numerous cycles did not reveal a pattern. The solution to these ambiguities is shown in Fig. 7. Figure 7(a) shows a rocking curve over a wide angular range for one of the strong structural reflections of the primary Ru1222 phase. For a properly randomized powder, of course, the observed intensity should be independent of the sample rotation, apart from absorption effects (neutron path length considerations) for the pellet itself. This is what is observed; the gradual intensity variation is due to the changing neutron path length in the pellet, with the minima occurring when the incident, or scattered, neutron path is parallel to the pellet. For the magnetic peak, on the other hand, we observe a very sharp peak, typical of a rocking curve for single crystal as shown in Fig. 7(b). Here the “background” is ~ 35 counts/min, and then we see one sharp peak well above this. We remark that, in hindsight, we found these single crystal peaks have a preferred orientation with respect to the pellet, and typically in these triple-axis diffraction measurements the pellet was oriented to (approximately) bisect the incident and scattered beams. Hence it was serendipitous that we usually found a magnetic peak. Indeed, Fig. 7(c) shows that the intensity is also strongly dependent on the tilt; the resolution in the vertical direction is quite coarse and this width is again comparable to the resolution. Then tiny shifts in the orientation of the pellet with thermal cycling caused substantial changes in intensity. The clear and unambiguous summary conclusion is that the magnetic scattering originates from single crystals of an impurity phase embedded in the pellet. Since the Ru1222 phase is polycrystalline in nature, this is further compelling evidence that the magnetic ordering cannot be associated with this phase.

Finally, we remark that we undertook two additional types of measurements. One was to measure the transmission of polarized neutrons through the sample, as we had done for the Ru1212 system,⁴ to search for a possible magnetic signal. The beam size was narrowed to a few mm in size to assure that all neutrons passed through the pellet, and to reduce the overall intensity on the detector. In our first measurement we found a small flipping ratio ($R \sim 3$) at low T , which increased up to the instrumental flipping ratio above ~ 60 K. This change in the flipping ratio suggested that there could be a ferromagnetic component associated with the magnetic ordering. No other change in transmitted polarization was detected up to room temperature. These data were collected before we had identified that the magnetic ordering originated from a single crystalline impurity phase. A later polar-

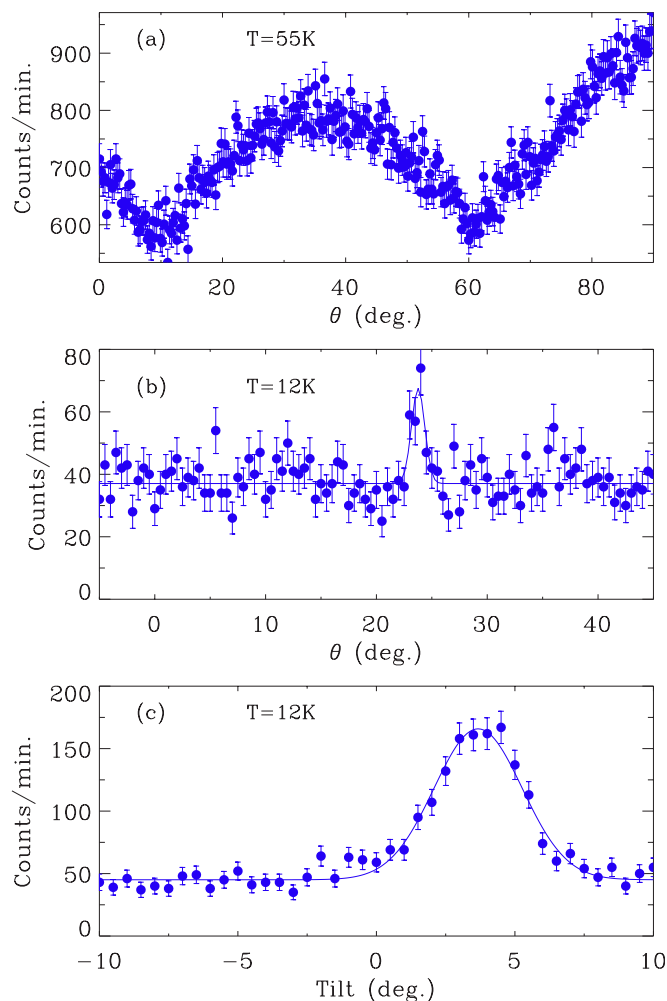


FIG. 7. (Color online) (a) Rocking curve over a wide angular range for one of the strong reflections of the primary Ru1222 phase. The gradual intensity variation originates from neutron absorption in the pellet due to the changing neutron path length in the pellet, with the minima occurring when the incident or scattered neutron path is parallel to the pellet. (b) Intensity of the magnetic peak as a function of sample rotation, which shows a very sharp peak, typical of a single crystal. We found that these single crystal peaks have a preferred orientation with respect to the pellet. (c) Intensity of one of the magnetic impurity peaks as the sample is tilted. The single crystal nature of the magnetic impurity contrasts with the polycrystalline nature of the Ru1222 phase, demonstrating that the magnetic ordering cannot be associated with the primary phase.

ized neutron transmission measurement again found the instrumental flipping ratio ($R \sim 26$) at elevated temperatures, and a quite small change in the flipping ratio below ~ 60 K. This “inconsistency” again is probably due to the serendipitous orientation of the magnetically ordered single crystals in the pellet, but we also note that the magnetic structure of the impurity may in fact possess a net magnetization. Finally, we note that we carried out a polarized transmission measurement on the NG-1 reflectometer on the sample after it had been crushed into a powder. The instrumental flipping ratio was ~ 50 , and no change in the flipping ratio was observed from room temperature to ~ 6 K.

One other measurement we carried out was to apply a magnetic field to the sample in an attempt to detect an induced moment in the system, as we have done on numerous other magnetic superconductors¹⁷ including the Ru1212.⁴ Data were collected for temperatures from 4 to 100 K and fields up to 7 T. No induced magnetic moment was detected on the Ru1222 structural peaks. Statistically we can put a limit of $\sim 0.25 \mu_B$ on any induced Ru moment in the system in this temperature range.

IV. DISCUSSION

Our initial magnetic diffraction measurements on this sample quickly revealed a magnetic ordering in the system, and promised a swift determination of the basic magnetic structure. However, the inconsistent intensities on thermal cycling and the paucity of magnetic peaks suggested the possible formation of an exotic cooperative state, such as a spontaneous vortex lattice. Subsequent extensive neutron measurements did indeed reveal a rather unexpected, but not exotic, situation; a significant fraction of a magnetic impurity phase has formed in the system during preparation, and this phase exists as single crystals with a distinct preferred orientation with respect to the pellet. Full high resolution diffraction analysis of the crushed pellet indicates that $\sim 13\%$ of the sample consists of impurity phases. However, the small sample size and complexity of the sample and associated diffraction pattern does not allow a detailed determination of these impurity phases, and therefore we cannot relate the observed magnetic ordering to a particular impurity. It should be noted, however, that the polarized neutron transmission measurements did not observe any ferromagnetic or-

dering around the Curie temperature (160 K) of (pure) SrRuO₃, so it appears that the 1:1:3 impurity is not this composition.

There have been a variety of magnetic transitions reported in the literature for this Ru1222 system. Our results make it clear that at least some of these are associated with impurities rather than the primary superconductor phase. For example, a magnetic transition of 77.6 K has been reported for a sample of Eu_{1.4}Ce_{0.6}RuSr₂Cu₂O₁₀ using muon spin rotation and magnetization measurements.³⁵ These are excellent techniques to investigate magnetic order, but they do not provide information about what structural phase is actually producing the order. This ordering closely matches our impurity ordering of 59 K (particularly given that the rare earth compositions are not identical), and this close proximity strongly suggests that the phase that is ordering is an impurity and not the Eu_{1.4}Ce_{0.6}RuSr₂Cu₂O₁₀ material. Their results also indicate that there is no interaction of this magnetic order with the superconductivity, which is also consistent with impurity phase ordering in the material. The nature of the magnetism, and possible magnetic ordering, in this ruthenate-cuprate system unfortunately remains an unresolved issue, but we hope that the present results help in clarifying and correctly identifying the various magnetic transitions that have been reported in this system.

ACKNOWLEDGMENTS

We would like to thank C. F. Majkrzak for his assistance on the NG-1 reflectometer, and J. L. Tallon and J. Budnick for stimulating discussions. Funding in New Zealand supported by the New Zealand Marsden Fund and the Royal Society of New Zealand.

-
- ¹L. Bauernfeind, W. Widder, and H. F. Braun, *Physica C* **254**, 151 (1995); *J. Low Temp. Phys.* **105**, 1605 (1996).
- ²I. Felner, U. Asaf, Y. Levi, and O. Millo, *Phys. Rev. B* **55**, R3374 (1997).
- ³I. Felner, U. Asaf, S. D. Goren, and C. Korn, *Phys. Rev. B* **57**, 550 (1998).
- ⁴J. W. Lynn, B. Keimer, C. Ulrich, C. Bernhard, and J. L. Tallon, *Phys. Rev. B* **61**, R14964 (2000).
- ⁵I. Felner, U. Asaf, Y. Levi, and O. Millo, *Physica C* **334**, 141 (2000).
- ⁶Y. Y. Xue, D. H. Cao, B. Lorenz, and C. W. Chu, *Phys. Rev. B* **65**, 020511(R) (2001).
- ⁷I. Felner, U. Asaf, F. Ritter, P. W. Klamut, and B. Dabrowski, *Physica C* **364**, 368 (2001).
- ⁸G. V. M. Williams and M. Ryan, *Phys. Rev. B* **64**, 094515 (2001).
- ⁹A. Fainstein, R. G. Pregeliasco, G. V. M. Williams, and H. J. Trodahl, *Phys. Rev. B* **65**, 184517 (2002).
- ¹⁰A. C. McLaughlin, J. P. Attfield, U. Asaf, and I. Felner, *Phys. Rev. B* **68**, 014503 (2003).
- ¹¹C. A. Cardoso, F. M. Araujo-Moreira, V. P. S. Awana, E. Takayama-Muromachi, O. F. de Lima, H. Yamauchi, and M. Karppinen, *Phys. Rev. B* **67**, 020407(R) (2003).
- ¹²V. P. S. Awana, M. A. Ansari, A. Gupta, R. B. Saxena, H. Kishan, D. Buddhikot, and S. K. Malik, *Phys. Rev. B* **70**, 104520 (2004).
- ¹³C. A. Cardoso, A. J. C. Lanfredi, A. J. Chiquito, F. M. Araujo-Moreira, V. P. S. Awana, H. Kishan, R. L. de Almeida, and O. F. de Lima, *Phys. Rev. B* **71**, 134509 (2005).
- ¹⁴I. Felner, E. Galstyan, and I. Nowik, *Phys. Rev. B* **71**, 064510 (2005).
- ¹⁵V. P. S. Awana, R. Lal, H. Kishan, A. V. Narlikar, M. Peurla, and R. Laiho, *Phys. Rev. B* **73**, 014517 (2006).
- ¹⁶For a recent review, see T. Nachtrab, C. Bernhard, C. T. Lin, D. Koelle, and R. Kleiner, *C. R. Phys.* **7**, 68 (2006).
- ¹⁷J. W. Lynn and S. Skanthakumar, in *Handbook on the Physics and Chemistry of Rare Earths*, edited by K. A. Gschneidner, Jr., L. Eyring, and M. B. Maple (North Holland, Amsterdam, 2001), Vol. 31, Chap. 199, pp. 315–350.
- ¹⁸A. Ono, *Jpn. J. Appl. Phys.* **34**, L1121 (1995).
- ¹⁹I. Zivkovic, Y. Hirai, B. H. Frazer, M. Prester, D. Drobac, D. Ariosa, H. Berger, D. Pavuna, G. Margaritondo, I. Felner, and M. Onellion, *Phys. Rev. B* **65**, 144420 (2002); Y. Hirai, I. Zivkovic, B. H. Frazer, A. Reginelli, L. Perfetti, D. Ariosa, G. Margaritondo, M. Prester, D. Drobac, D. T. Jiang, Y. Hu, T. K. Sham, I. Felner, M. Pederson, and M. Onellion, *ibid.* **65**, 054417 (2002).

- ²⁰Y. Y. Xue, B. Lorenz, D. H. Cao, and C. W. Chu, *Phys. Rev. B* **67**, 184507 (2003).
- ²¹I. Felner, E. Galstyan, R. H. Herber, and I. Nowik, *Phys. Rev. B* **70**, 094504 (2004).
- ²²G. V. M. Williams, H. K. Lee, and S. K. Goh, *Phys. Rev. B* **71**, 014515 (2005); S. K. Goh, G. V. M. Williams, E. K. Hemery, and H. K. Lee, *ibid.* **74**, 134506 (2006).
- ²³G. V. M. Williams, *Phys. Rev. B* **73**, 064510 (2006).
- ²⁴D. G. Naugle, K. D. D. Rathnayaka, V. B. Krasovitsky, B. I. Belevtsev, M. P. Analska, G. Agnolet, and I. Felner, *J. Appl. Phys.* **99**, 08M501 (2006).
- ²⁵I. Zivkovic, D. Pajic, and K. Zadro, *Physica C* **452**, 16 (2007).
- ²⁶A. Larson and R. B. Von Dreele (unpublished).
- ²⁷See, for example, V. P. S. Awana, R. Tripaathi, V. K. Sharma, H. Kishan, E. Takayama-Muromachi, and I. Felner, eprint arXiv:cond-mat/0610325 (unpublished).
- ²⁸N. E. Brese and M. O'Keeffe, *Acta Crystallogr., Sect. B: Struct. Sci.* **47**, 192 (1991).
- ²⁹A. C. McLaughlin, W. Zhou, J. P. Attfield, A. N. Fitch, and J. L. Tallon, *Phys. Rev. B* **60**, 7512 (1999).
- ³⁰H. Zhang, J. W. Lynn, W-H. Li, T. W. Clinton, and D. E. Morris, *Phys. Rev. B* **41**, 11229 (1990).
- ³¹See, for example, J. W. Lynn, L. Vasiliu-Doloc, and M. A. Subramanian, *Phys. Rev. Lett.* **80**, 4582 (1998); C. P. Adams, J. W. Lynn, V. N. Smolyaninova, A. Biswas, R. L. Greene, W. Ratcliff II, S-W. Cheong, Y. M. Mukovski, and D. A. Shulyatev, *Phys. Rev. B* **70**, 134414 (2004).
- ³²S. -M. Choi, J. W. Lynn, D. Lopez, P. L. Gammel, P. C. Canfield, and S. L. Bud'ko, *Phys. Rev. Lett.* **87**, 107001 (2001).
- ³³J. W. Lynn, J. L. Ragazzoni, R. Pynn, and J. Joffrin, *J. Phys. (France) Lett.* **42**, L45 (1981); J. W. Lynn, G. Shirane, W. Thomlinson, and R. N. Shelton, *Phys. Rev. Lett.* **46**, 368 (1981); J. W. Lynn, J. A. Gotaas, R. W. Erwin, R. A. Ferrell, J. K. Bhattacharjee, R. N. Shelton, and P. Klavins, *ibid.* **52**, 133 (1984).
- ³⁴See, for example, J. W. Lynn, S. Skanthakumar, Q. Huang, S. K. Sinha, Z. Hossain, L. C. Gupta, R. Nagarajan, and C. Godart, *Phys. Rev. B* **55**, 6584 (1997).
- ³⁵A. Shengelaya, R. Khasanov, D. G. Eschenko, I. Felner, U. Asaf, I. M. Savic, H. Keller, and K. A. Muller, *Phys. Rev. B* **69**, 024517 (2004).